

# FUSION ARCHITECTURES FOR 3D TARGET TRACKING USING IRST AND RADAR MEASUREMENTS

VPS Naidu\*

## Abstract

*Seven different architectures are presented to fuse IRST and radar data to track the target in 3D Cartesian coordinates, with the measurements available in polar coordinates. Performance of these architectures is checked with simulated data. Detailed mathematical expressions are provided which could be useful for algorithm implementation. From this study, it is concluded that CM (Common Measurements) architecture gives state estimates with relatively less uncertainty followed by SVF (State Vector Fusion). IRST gives target states with relatively high uncertainty followed by radar. This shows the necessity of the fusion in tracking system. In all, CM architecture is very simple, easy to implement and can be used in real time.*

## Introduction

Modern military aircraft are equipped with diverse sensors in order to aid the pilot. If these sensors are perfect then the target tracking could be achieved with simple geometry. In general, sensors are not perfect and their measurements are corrupted with noise. Moreover, single sensor may not provide all the information about the target. Hence, filters and multiple sensors are used to enhance the target tracking capabilities. Radar can measure azimuth, elevation and range of a target. It can measure range with good resolution, but the angular measurements are not so accurate. Despite this, radar provides sufficient information to track the target. The uncertainty associated with radar might be represented as a volume whose dimensions are relatively large perpendicular to the measured line of sight and small along the line of sight. An infrared search and track sensor (IRST) can measure azimuth and elevation of a target with good resolution. It can provide the direction of a target but not its location because it does not measure the range. The uncertainty associated with IRST might be represented as a square whose dimensions are comparatively small perpendicular to the measured line of sight. By fusing the measurements from radar and IRST, the resultant uncertainty of the estimated position of the target would be smaller than the uncertainty of either of the measurements alone. An improved estimate of target location and reduced positional uncertainty would result from the fusion of information obtained from multi sources [1-3].

This paper deals with tracking of target in 3D Cartesian coordinates by fusing measurements from IRST and radar in polar coordinates. Extended Kalman filter is used to estimate the state of a target using target motion and measurement models. In this paper, seven different fusion architectures are evaluated for the above purpose. The performance of these algorithms is presented in terms of percentage of fit error (PFE), root mean square error in position (RMSPE), root sum square error in position (RSSPE) and mean absolute state error (MAE).

## Extended Kalman Filter

A general motion model used in discrete extended Kalman filter for target tracking is [1, 3, 4] :

$$X(k) = FX(k-1) + Gw(k-1) \quad (1)$$

$$z(k) = h(X(k)) + v(k) \quad (2)$$

where  $X(k)$  is the state vector,  $F$  is the state transition matrix and  $G$  is the process noise gain matrix. The process noise  $w(k)$  and the measurement noise  $v(k)$  are zero-mean, mutually independent, white, Gaussian with covariance  $Q$  and  $R$  respectively.  $z(k)$  is the measurement vector at time  $k$  and  $h(X(k))$  is a nonlinear function of the states computed at time  $k$ .

Linear Kalman filter could be used for target tracking if the states and the measurements are in Cartesian coor-

\* Scientist, Multi Sensor Data Fusion Lab, Flight Mechanics and Control Division (FMCD), National Aerospace Laboratories, Kodihalli, Bangalore-560 017, India, Email : vpsnaidu@css.nal.res.in

Manuscript received on 07 Sep 2009; Paper reviewed, revised and accepted as a Full Length Contributed Paper on 10 May 2010

dinate system. Radar and IRST provide the measurements in a spherical/polar coordinate system. In most cases the state vector is to be estimated in Cartesian coordinate system. Eq. (2) is nonlinear and it needs to be linearised to fit into the Kalman filter framework entailing the use of extended Kalman filter (EKF).

### State Prediction

The state and state covariance matrix at time  $k-1$  are predicted to time  $k$  as follows :

$$\begin{aligned}\tilde{X}(k|k-1) &= F \hat{X}(k-1|k-1) \\ \tilde{P}(k|k-1) &= F \hat{P}(k-1|k-1) F^T + G Q G^T\end{aligned}\quad (3)$$

where  $\hat{X}$  is the estimated state vector,  $\hat{P}$  is the estimated state covariance matrix,  $\tilde{X}$  is the predicted state and  $\tilde{P}$  is the predicted state covariance matrix.

### Measurement Update

Innovation :

$$e(k) = z(k) - \tilde{z}(k|k-1) \quad (4)$$

Innovation covariance :

$$S = H(k) \tilde{P}(k|k-1) H(k)^T + R \quad (5)$$

where  $\tilde{z}(k|k-1)$  is the predicted measurement and  $H(k)$  is the linearised measurement matrix. The measurement update part consists of the following equations.

Filter gain :

$$K(k) \tilde{P}(k|k-1) H(k)^T S^{-1} \quad (6)$$

Updated state :

$$\hat{X}(k|k) = \tilde{X}(k|k-1) + K(k) e(k) \quad (7)$$

Updated state covariance :

$$\hat{P}(k|k) = [I - K(k) H(k)] \tilde{P}(k|k-1) \quad (8)$$

### Predicted Measurement and Linearized Measurement Matrix

Finite difference method is used to compute the linearized measurement matrix. Consider the state vector consisting of position, velocity and acceleration components in x-, y- and z-direction as

sisting of position, velocity and acceleration components in x-, y- and z-direction as

$$[x \quad \dot{x} \quad \ddot{x} \quad y \quad \dot{y} \quad \ddot{y} \quad z \quad \dot{z} \quad \ddot{z}] \quad (9)$$

The predicted state is in the form :

$$[\tilde{x} \quad \tilde{\dot{x}} \quad \tilde{\ddot{x}} \quad \tilde{y} \quad \tilde{\dot{y}} \quad \tilde{\ddot{y}} \quad \tilde{z} \quad \tilde{\dot{z}} \quad \tilde{\ddot{z}}] = \tilde{X}(k|k-1) \quad (10)$$

The predicted measurement when the measurement vector consists of only azimuth and elevation is :

$$\tilde{z}(k|k-1) = h[\tilde{X}(k|k-1)] = [\tilde{\theta} \quad \tilde{\phi}]^T \quad (11)$$

The predicted measurement when the measurement vector consists of azimuth, elevation and range is :

$$\tilde{z}(k|k-1) = h[\tilde{X}(k|k-1)] = [\tilde{\theta} \quad \tilde{\phi} \quad \tilde{r}]^T \quad (12)$$

Components in the predicted measurement are computed from the predicted state vector given in Eq. (10).

$$\tilde{\theta} = \tan^{-1} \left( \frac{\tilde{y}}{\tilde{x}} \right), \quad (13)$$

$$\tilde{\phi} = \tan^{-1} \left( \frac{\tilde{z}}{\sqrt{\tilde{x}^2 + \tilde{y}^2}} \right), \quad (14)$$

$$\tilde{r} = \sqrt{\tilde{x}^2 + \tilde{y}^2 + \tilde{z}^2} \quad (15)$$

### Finite Difference Method [3, 4]

Calculation of linearized measurement matrix can be accomplished by the finite difference method. This method is generalised and flexible.

$$H(k) = H_{ij} = \frac{\partial h_i}{\partial x_j} \Big|_{x=\tilde{X}(k|k-1)} = \frac{h_i(x_j + \Delta x_j) - h_i(x_j)}{\Delta x_j} \quad (16)$$

where

$i = 1, 2, \dots$ , length of the measurement vector

$j = 1, 2, \dots$ , length of the state vector

$\Delta x_j$  = perturbation step size

For small perturbation  $\Delta x$  in each of the unknown variables, the perturbed value  $h_i(x_j + \Delta x_j)$  is computed.

The corresponding elements of  $H_{ij}$  are given by the finite difference in the function  $h$  (Eq. 2) to changes in that state. In general a perturbation step size of  $10^{-7}$  is considered to be adequate.

### Fusion of IRST and Radar Data

In this section six different architectures are presented to fuse IRST and radar data to track the target in 3D Cartesian coordinates, where the measurements from radar and IRST are in polar coordinates.  $z_i(k) = [\theta_i \ \varphi_i]^T$  and  $z_r(k) = [\theta_r \ \varphi_r \ r_r]^T$  denote the measurements from IRST and radar respectively.

Noise covariance matrix of IRST is :

$$R_i = \begin{bmatrix} i\sigma_\theta^2 & 0 \\ 0 & i\sigma_\varphi^2 \end{bmatrix}$$

Noise covariance matrix of radar is :

$$R_r = \begin{bmatrix} r\sigma_\theta^2 & 0 & 0 \\ 0 & r\sigma_\varphi^2 & 0 \\ 0 & 0 & r\sigma_r^2 \end{bmatrix}$$

### Selective Measurements (SM)

In this architecture (Fig.1), the measurement vector consists of selective measurements from radar and IRST. The measurement vector consists of azimuth and elevation measurements taken from IRST and range measurement taken from radar. Similarly, the measurement covariance matrix is formed. It is simple EKF filter and the equations required to implement the tracking algorithm are as follows :

State Prediction :

$$\begin{aligned} \tilde{X}(k|k-1) &= F \hat{X}(k-1|k-1) \\ \tilde{P}(k|k-1) &= F \hat{P}(k-1|k-1) F^T + G Q G^T \end{aligned} \quad (17)$$

Fusion :

$$z(k) = [\theta_i \ \varphi_i \ r_r]^T$$

$$R = \begin{bmatrix} i\sigma_\theta^2 & 0 & 0 \\ 0 & i\sigma_\varphi^2 & 0 \\ 0 & 0 & r\sigma_r^2 \end{bmatrix} \quad (18)$$

Measurement updation :

$$\begin{aligned} H &= h(\tilde{X}(k|k-1)) \\ \tilde{z}(k|k-1) &= H \tilde{X}(k|k-1) \\ e &= z(k) - \tilde{z}(k|k-1) \\ S &= H \tilde{P}(k|k-1) H^T + R \\ K &= \tilde{P}(k|k-1) H^T S^{-1} \\ \hat{X}(k|k) &= \tilde{X}(k|k-1) + Ke \\ \hat{P}(k|k) &= [I - KH] \tilde{P}(k|k-1) \end{aligned} \quad (19)$$

### Measurement Fusion (MF) [6, 7]

In this architecture (Fig.2), the measurement vector consists of fused azimuth, fused elevation and range taken from radar. Similarly, the measurement covariances for azimuth and elevation from IRST and radar are fused and measurement noise covariance for range is taken from radar. The fused azimuth is obtained by fusing the azimuths coming from IRST and radar. Similarly, the fused elevation is obtained by fusing the elevations coming from IRST and radar. Instead of fusing the measurement in the use of EKF, the measurements from IRST and radar are merged into an augmented measurement vector and measurement noise variances from both sensors also concatenated to produce the same results [6].

State Prediction : (Eq. 17)

Fusion :

$$\begin{aligned} z_d(k) &= [\theta_r \ \varphi_r]^T \\ R_d &= \begin{bmatrix} r\sigma_\theta^2 & 0 \\ 0 & r\sigma_\varphi^2 \end{bmatrix} \end{aligned}$$

$$\begin{aligned}
z_f &= z_i(k) + z_i(k) \left[ R_i + R_d \right]^{-1} (z_d(k) - z_i(k)) \\
R_f &= R_i - R_i \left[ R_i + R_d \right]^{-1} R_i \\
z(k) &= \begin{bmatrix} z_f(1) & z_f(2) & r_r \end{bmatrix}^T \\
R &= \begin{bmatrix} R_f(1,1) & 0 & 0 \\ 0 & R_f(2,2) & 0 \\ 0 & 0 & r_r \sigma_r^2 \end{bmatrix} \quad (20)
\end{aligned}$$

Measurement updation : (Eq. 19)

### State Vector Fusion (SVF) [3, 6-10]

In this architecture (Fig.3), tracks are found with IRST and radar measurements separately and the resultant state vectors (tracks) are fused to get final target state estimations. Similarly, the state error covariances of the individual tracks are fused to get the final state error covariance matrix.

State Prediction :

$$\begin{aligned}
\tilde{X}_i(k|k-1) &= F \hat{X}_i(k-1|k-1) \\
\tilde{P}_i(k|k-1) &= F \hat{P}_i(k-1|k-1) F^T + G Q G^T \quad (21a)
\end{aligned}$$

$$\begin{aligned}
\tilde{X}_r(k|k-1) &= F \hat{X}_r(k-1|k-1) \\
\tilde{P}_r(k|k-1) &= F \hat{P}_r(k-1|k-1) F^T + G Q G^T \quad (21b)
\end{aligned}$$

Measurement updation :

$$\begin{aligned}
H_i &= h(\tilde{X}_i(k|k-1)) \\
\tilde{z}_i(k|k-1) &= H_i \tilde{X}_i(k|k-1) \\
e_i &= z_i - \tilde{z}_i(k|k-1) \\
S_i &= H_i \tilde{P}_i(k|k-1) H_i^T + R_i \\
K_i &= \tilde{P}_i(k|k-1) H_i^T S_i^{-1}
\end{aligned}$$

$$\begin{aligned}
\hat{X}_i(k|k) &= \tilde{X}_i(k|k-1) + K_i e_i \\
\hat{P}_i(k|k) &= [I - K_i H_i] \tilde{P}_i(k|k-1) \quad (22a)
\end{aligned}$$

$$\begin{aligned}
H_r &= h(\tilde{X}_r(k|k-1)) \\
\tilde{z}_r(k|k-1) &= H_r \tilde{X}_r(k|k-1) \\
e_r &= z_r - \tilde{z}_r(k|k-1)
\end{aligned}$$

$$S_r = H_r \tilde{P}_r(k|k-1) H_r^T + R_r$$

$$K_r = \tilde{P}_r(k|k-1) H_r^T S_r^{-1}$$

$$\begin{aligned}
\hat{X}_r(k|k) &= \tilde{X}_r(k|k-1) + K_r e_r \\
\hat{P}_r(k|k) &= [I - K_r H_r] \tilde{P}_r(k|k-1) \quad (22b)
\end{aligned}$$

Fusion :

$$\begin{aligned}
\hat{X}_f(k|k) &= \hat{X}_i(k|k) + \hat{P}_i(k|k) \left[ \hat{P}_i(k|k) + \hat{P}_r(k|k) \right]^{-1} \\
&\quad \left( \hat{X}_r(k|k) - \hat{X}_i(k|k) \right) \\
\hat{P}_f(k|k) &= \hat{P}_i(k|k) + \hat{P}_i(k|k) \\
&\quad \left( \hat{P}_i(k|k) + \hat{P}_r(k|k) \right)^{-1} \hat{P}_i^T(k|k) \quad (23)
\end{aligned}$$

### Feedback SVF (FSVF) [6, 11]

In this architecture (Fig.4), the fused state vector and state error covariance matrix are feedback to a single state predictor and the out put of this is fed to two measurement updation. IRST measurements are used at one of the measurement updation to estimate the target states and radar measurements are used at the other measurement updation to estimate the target states. Finally the estimates are fused and then feedback to the prediction.

State Prediction :

$$\tilde{X}(k|k-1) = F \hat{X}_f(k-1|k-1)$$

$$\tilde{P}(k|k-1) = F \hat{P}_f(k-1|k-1) F^T + G Q G^T \quad (24)$$

Measurement Update : (Eq. 22)

Fusion :

$$P_{ir}(k|k) = P_{ri}^T(k|k) = [I - K_i(k) H_i(k)] \tilde{P}(k|k-1) [I - K_r(k) H_r(k)]^T \quad (25)$$

$$\hat{X}_f(k) = \hat{X}_i(k|k) + [\hat{P}_i(k|k) - \hat{P}_{ir}(k|k)] [\hat{P}_i(k|k) + \hat{P}_r(k|k) - \hat{P}_{ir}(k|k) - \hat{P}_{ri}(k|k)]^{-1} (\hat{X}_r(k|k) - \hat{X}_i(k|k)) \quad (26)$$

$$\hat{P}_f(k|k) = \hat{P}_i(k|k) - [\hat{P}_i(k|k) - \hat{P}_{ir}(k|k)] [\hat{P}_i(k|k) + \hat{P}_r(k|k) - \hat{P}_{ir}(k|k) - \hat{P}_{ri}(k|k)]^{-1} [\hat{P}_i(k|k) - \hat{P}_{ir}(k|k)] \quad (27)$$

### Predicted SVF (PSVF) [6]

In this architecture (Fig.5), the predicted state vectors from IRST and radar are fused. Similarly, the predicted state error covariances are also fused. The fused estimates are feed to two measurement update. IRST measurements are used in one of the measurement update to estimate the target states and radar measurements are used in the other measurement update to estimate the target states. These estimates are feedback to the respective prediction stage and also fused to get the final target estimates.

State Prediction : (Eq. 21)

$$\tilde{P}_{ir}(k|k-1) = \tilde{P}_{ri}^T(k|k-1) = F \hat{P}_{ir}(K-1|k-1) F^T + G Q G^T \quad (28)$$

Fusion : (at predicted stage)

$$\tilde{X}(k|k-1) = \tilde{X}_i(k|k-1) + [\tilde{P}_i(k|k-1) - \tilde{P}_{ir}(k|k-1)]$$

$$[\tilde{P}_i(k|k-1) + \tilde{P}_r(k|k-1) - \tilde{P}_{ir}(k|k-1) - \tilde{P}_{ri}(k|k-1)]^{-1} (\tilde{X}_r(k|k-1) - \tilde{X}_i(k|k-1)) \quad (29)$$

$$\tilde{P}(k|k-1) = \tilde{P}_i(k|k-1) - [\tilde{P}_i(k|k-1) - \tilde{P}_{ir}(k|k-1)] [\tilde{P}_i(k|k-1) + \tilde{P}_r(k|k-1) - \tilde{P}_{ir}(k|k-1) - \tilde{P}_{ri}(k|k-1)]^{-1} [\tilde{P}_i(k|k-1) - \tilde{P}_{ir}(k|k-1)] \quad (30)$$

Measurement update : (Eq. 22)

$$\hat{P}_{ir}(k|k) = \hat{P}_{ri}^T(k|k) = [I - K_i(k) H_i(k)] \tilde{P}(k|k-1) [I - K_r(k) H_r(k)]^T \quad (31)$$

Fusion : (at estimated stage)

$$X(k) = \hat{X}_i(k|k) + [\hat{P}_i(k|k) - \hat{P}_{ir}(k|k)] [\hat{P}_i(k|k) + \hat{P}_r(k|k) - \hat{P}_{ir}(k|k) - \hat{P}_{ri}(k|k)]^{-1} (\hat{X}_r(k|k) - \hat{X}_i(k|k)) \quad (32)$$

$$P(k|k) = \hat{P}_i(k|k) - [\hat{P}_i(k|k) - \hat{P}_{ir}(k|k)] [\hat{P}_i(k|k) + \hat{P}_r(k|k) - \hat{P}_{ir}(k|k) - \hat{P}_{ri}(k|k)]^{-1} [\hat{P}_i(k|k) - \hat{P}_{ir}(k|k)] \quad (33)$$

### Decentralized Kalman Filter (DKF) [12-14]

In this algorithm, the states obtained from local Kalman filters (LKF) are fed to the global Kalman filter (GKF) for final target estimates as shown in Fig.6. One of the local KF utilizes IRST measurements and another local KF utilizes radar measurements. The LKFs transmit only the state error information ( $\hat{X}_i(k)$  and  $\hat{X}_r(k)$ ) and covariance error information ( $\hat{P}_i(k)$  and  $\hat{P}_r(k)$ ) to the GKF. The GKF have state prediction and estimate correction

instead of measurement updation. At each local EKF the following quantities has to be computed and then passed to the global EKF. The state and covariance error information are utilized at estimate correction stage to obtain final target estimates.

#### At LKF : (Using IRST Measurements)

State Prediction : (Eq. 19a)

Measurement Updation : (Eq. 22a)

$$\begin{aligned}\hat{X}_i(k) &= \hat{P}_i^{-1}(k|k) \hat{X}_i(k|k) - \tilde{P}_i^{-1}(k|k-1) \tilde{X}_i^{-1}(k|k-1) \\ \hat{P}_i(k) &= \hat{P}_i^{-1}(k|k) - \tilde{P}_i^{-1}(k|k-1)\end{aligned}\quad (34)$$

#### At LKF : (Using Radar Measurements)

State Prediction : (Eq. 19b)

Measurement Updation : (Eq. 22a)

$$\begin{aligned}\hat{X}_r(k) &= \hat{P}_r^{-1}(k|k) \hat{X}_r(k|k) - \tilde{P}_r^{-1}(k|k-1) \tilde{X}_r(k|k-1) \\ \hat{P}_r(k) &= \hat{P}_r^{-1}(k|k) - \tilde{P}_r^{-1}(k|k-1)\end{aligned}\quad (35)$$

Fusion : (at GKF)

State Prediction :

$$\begin{aligned}\tilde{X}(k|k-1) &= F \hat{X}(k-1|k-1) \\ \tilde{P}(k|k-1) &= F \hat{P}(k-1|k-1) F^T + G Q G^T\end{aligned}\quad (36)$$

Estimate Correction :

$$\begin{aligned}\hat{P}^{-1}(k|k) &= \tilde{P}^{-1}(k|k-1) + \hat{P}_i^{-1}(k) + \hat{P}_r^{-1}(k) \\ \hat{X}(k|k) &= \hat{P}(k|k) \left[ \tilde{P}^{-1}(k|k-1) \tilde{X}(k|k-1) + \hat{X}_i^{-1}(k) + \hat{X}_r^{-1}(k) \right]\end{aligned}\quad (37)$$

#### Common Measurements (CM)

In this algorithm, the range obtained from the radar is considered as an additional measurement in IRST tracker and the rest of the procedure is very similar to SVF.

State Prediction : (Eq. 21)

Measurement Updation : (Eq. 22)

where

$$z_i(k) = [\theta_i \ \phi_i \ r_r]^T$$

$$R_i = \begin{bmatrix} \sigma_{\theta}^2 & 0 & 0 \\ 0 & \sigma_{\phi}^2 & 0 \\ 0 & 0 & \sigma_{r_r}^2 \end{bmatrix}\quad (38)$$

Fusion : (Eq. 23)

#### Radar

In this algorithm, the radar measurements are as it is taken in tracker algorithm.

State Prediction : (Eq. 21b)

Measurement Updation : (Eq. 22b)

Fusion : Nil

#### IRST

In this algorithm, the IRST measurements are as it is taken in tracker algorithm.

State Prediction : (Eq. 21a)

Measurement Updation : (Eq. 22a)

Fusion : Nil

#### Numerical Simulation and Discussion

The 3DOF kinematic model, with position, velocity and acceleration components in each of the three Cartesian coordinates x, y and z has the following transition and process noise gain matrices.

$$F = \text{diag} [\Phi \ \Phi \ \Phi] \quad G = \text{diag} [\zeta \ \zeta \ \zeta] \quad (39)$$

where

$$\Phi = \begin{bmatrix} 1 & T & T^2/2 \\ 0 & 1 & T \\ 0 & 0 & 1 \end{bmatrix}$$

$$\zeta = \begin{bmatrix} T^3/6 \\ T^2/2 \\ T \end{bmatrix}$$

where  $T$  is the sampling interval,  $F$  is the state transition matrix and  $G$  is the process noise gain matrix.

Simulation utilizes the following parameters :

Sampling interval : 0.1 sec.

Process noise variance :  $1^2$

Measurement noise variance :

Sensor	Azimuth (rad)	Elevation (rad)	Range (meters)
ISRT	$i \sigma_\theta^2 = 10^5$	$i \sigma_\phi^2 = 10^5$	-----
Radar	$r \sigma_\theta^2 = 10^2$	$i \sigma_\phi^2 = 10^2$	$r \sigma_r^2 = 100$

Duration of Simulation : 50 sec

Initial state vector is :

$$[x \ \dot{x} \ \ddot{x} \ y \ \dot{y} \ \ddot{y} \ z \ \dot{z} \ \ddot{z}]$$

$$= [10000 \ -200 \ 0.5 \ -1000 \ -100 \ -0.3 \ 1000 \ 1 \ 0.01]$$

The simulated noisy measurements in polar coordinates are shown in Fig.7.

The initial state vector is chosen as :

$$\hat{X}_0 = 0.9 X_t \quad (40)$$

$\hat{X}_0$  : initial estimated state vector at scan number one

$X_t$  : true state vector at scan number one

The expression for the initial state error covariance matrix is given by :

$$\hat{P}_0 = \text{diag} \left[ (X_t - \hat{X}_0)^2 \right] \quad (41)$$

The filter performance is checked by computing [3, 8] :

- The percentage fit error (PFE) in  $x$ ,  $y$  and  $z$  positions :

$$PFE_x = 100 * \frac{\text{norm}(x - \hat{x})}{\text{norm}(x)}, \quad (42)$$

similarly for  $y$  and  $z$  positions

- Root mean square error in position :

$$\text{RMSPE} = \sqrt{\frac{1}{N} \sum_{i=1}^N \frac{(x_i - \hat{x}_i)^2 + (y_i - \hat{y}_i)^2 + (z_i - \hat{z}_i)^2}{3}} \quad (43)$$

- Root sum square error in position :

$$\text{RSSPE} = \sqrt{(x - \hat{x})^2 + (y - \hat{y})^2 + (z - \hat{z})^2} \quad (44)$$

- Absolute error in (AE)  $x$ ,  $y$  and  $z$  positions :

$$A E_x(i) = |x(i) - \hat{x}(i)| \quad i = 1, 2, \dots, N, \quad (45)$$

similarly for  $y$  and  $z$  positions

- Mean absolute error in  $x$ ,  $y$  and  $z$  positions :

$$MAE_x = \frac{1}{N} \sum_{i=1}^N |x(i) - \hat{x}(i)|, \quad (46)$$

similarly for  $y$  and  $z$  positions

Performance of six fusion architectures is evaluated using fifty Monte Carlo simulations. The percentage fit error (PFE) in  $x$ -,  $y$ - and  $z$ -positions and root mean square errors in position, velocity and acceleration are shown in Table-1. Mean absolute error in  $x$ -,  $y$ - and  $z$ -position and their derivatives are shown in Table-2. The values shown in bold indicate the best results. The root sum errors in position, in velocity and in acceleration are shown in Fig.8a to 8e. Absolute error in  $x$ -,  $y$ - and  $z$ -positions, velocities and accelerations are shown in Fig.9a to 9e. From tables and Figs.8 to 9, it is observed that target tracking with either radar or IRST alone shows degraded performance than the fusion of radar and IRST. Among the fusion architectures, DKF performance is poor and SVF performance is better in velocity and acceleration estimates. Overall, SM performance is very good. Root sum variance and mean root sum variance related position, velocity & acceleration are shown in Fig.10a to 10e and Table-3. It is observed that, CM shows the lowest uncertainty followed by SVF and other architectures show high uncertainty in the state estimation. Uncertainty in state estimation is high in case of IRST followed by radar. This shows the necessity of fusion. The execution time for each algorithm is shown in Table-3. As expected, tracking with IRST alone take less time with degraded performance.

Table-1 : Percentage Fit Errors in x-, y- and z-Position						
Architecture	$PFE_x$	$PFE_y$	$PFE_z$	$RMSPE$	$RMSVE$	$RMSAE$
SM	0.7849	<b>0.1645</b>	0.7064	26.8011	4.2201	1.6642
MF	<b>0.7848</b>	0.1646	0.7069	26.8016	4.2212	1.6643
SVF	0.7853	0.1690	0.7039	26.8344	<b>4.1568</b>	<b>1.5962</b>
FSVF	0.7849	<b>0.1645</b>	0.7064	<b>26.8010</b>	4.2200	1.6642
PSVF	0.7849	0.1650	0.7064	26.8047	4.2210	1.6568
DKF	0.7858	0.1694	0.7102	26.8504	4.2891	1.6786
CM	0.7851	0.1658	<b>0.7023</b>	26.8089	4.1606	1.6259
Radar	1.5201	1.8006	8.8883	94.1222	15.7084	2.1539
IRST	8.5955	10.4367	8.7399	412.8613	27.8235	2.0938

Table-2 : Mean Absolute Errors in x-, y- and z-Position and their Derivatives									
Architecture	$MAE_x$	$MAE_y$	$MAE_z$	$MAE_{\dot{x}}$	$MAE_{\dot{y}}$	$MAE_{\dot{z}}$	$MAE_{\ddot{x}}$	$MAE_{\ddot{y}}$	$MAE_{\ddot{z}}$
SM	6.2516	4.8971	5.7275	3.3248	3.1440	3.1480	1.4134	1.2003	1.2890
MF	<b>6.2477</b>	<b>4.8967</b>	5.7331	3.3231	3.1456	3.1497	1.4131	1.2006	1.2893
SVF	6.4446	5.1984	5.6979	<b>3.3089</b>	3.1188	<b>3.0113</b>	<b>1.3668</b>	1.1387	1.2300
FSVF	6.2517	4.8967	5.7272	3.3248	3.1438	3.1479	1.4134	1.2003	1.2890
PSVF	6.2617	4.9204	5.7282	3.3531	3.1350	3.1470	1.4133	1.1797	1.2895
DKF	6.5143	5.2024	5.7673	3.3814	3.2423	3.1558	1.4195	1.2266	1.2905
CM	6.3464	4.9710	<b>5.6865</b>	3.3391	<b>3.0919</b>	3.0266	1.4328	<b>1.1339</b>	<b>1.2280</b>
Radar	59.4840	64.3281	88.0363	12.4612	9.8000	13.5268	1.9578	1.3344	1.7755
IRST	374.567	333.547	88.6799	21.4919	27.7802	5.4429	1.5139	1.9959	1.3313

Table-3 : Mean Root Sum Variance in Position, Velocity and Acceleration and Execution Time				
Architecture	MRSvarP	MRSvarV	MRSvarA	Execution Time (sec)
SM	13.0025	7.4623	3.1682	0.235
MF	12.9984	7.4609	3.1680	0.140
SVF	12.3922	6.5255	2.4869	0.266
FSVF	13.0025	7.4623	3.1682	0.437
PSVF	12.9530	7.3111	3.1666	0.609
DKF	12.7589	7.3729	3.1574	0.453
CM	<b>12.3031</b>	<b>6.2961</b>	<b>2.3782</b>	0.282
Radar	153.1945	29.1265	4.6902	0.125
IRST	709.1513	50.7274	4.9823	<b>0.110</b>



### Conclusion

Seven different architectures are presented to fuse IRST and radar data to track the target in 3D Cartesian coordinates, where the measurements are in polar coordinates. Their performance is evaluated with numerical simulation. Detailed mathematical expressions are given which could be useful for implementation. From the results it is concluded that CM architecture give state estimates with relatively less uncertainty followed by SVF architecture. Uncertainties in state estimates are more in case of IRST and followed by radar. This shows the necessity of the fusion.

### References

1. Samuel Blackman and Robert Popoli., "Design and Analysis of Modern Tracking Systems", Artech House, London, 1999.
2. David L. Hall and Sonya A. H. McMullen., "Mathematical Techniques in Multisensor Data Fusion", Second edition, Artech House, London, 2004.
3. Naidu, V.P.S., "Fusion of Radar and IRST Sensor Measurements for 3D Target Tracking using Extended Kalman Filter", Defence Science Journal, Vol. 59, No.2, pp.175-182, March 2009.
4. Yaakov Bar-Shalom and X. Li., "Estimation and Tracking: Principles, Techniques, and Softwares", Artech House, London, 1993.
5. Girija, G. and Christoph Zorn., "Flight Path Reconstruction for Sensor Failure Detection and Health Monitoring", NAL PD FC 0418, 2004.
6. Gao, J.B. and Harris, C.J., "Some Remarks on Kalman Filters for the Multisensor Fusion", Information Fusion, 3, pp.191-201, 2002.
7. Zhiqiang Hou and Chonghao Han., "A Target Tracking System Based on Radar and Image Fusion", International Conference on Information Fusion, Australia, pp. 1426-1432, 2003.
8. Naidu, V.P.S., Girija, G. and Raol, J.R., "Data Association and Fusion Algorithms for Tracking in presence of Measurement Loss", Journal of the Institution of Engineers (I), Vol. 86, pp.17-28, May 2005.
9. Saha, R.K., "Effect of Common Process Noise on Two-Sensor Track Fusion", J. of Gui and Dyn., Vol.19, No.4, pp.829-835, July 1996.
10. Roecker, J. and McGillem, C., "Comparison of Two-sensor Tracking Methods Based on State Vector Fusion and Measurement Fusion", IEEE Trans. on Aero. and Elec. Sys., 24(4), pp.447-449, 1988.
11. Blanc, C., Trassoudaine, L., Le Guilloux, Y. and Moreira, R., "Track to Track Fusion Method Applied to Road Obstacle Detection", International Conference on Information Fusion, Stockholm, Sweden, pp.775-782, 2004.
12. Rao, B.S.Y., Durrant-Whyte, H.F. and Sheen, J.A., "A Fully Decentralized Multi-Sensor System for racking and Surveillance", The International Journal of Robotics Research, 12(1), pp.20-44, 1993.
13. Hamid R. Hashemipour., Sumit Roy and Alan J. Laub., "Decentralized Structures for Parallel Kalman Filtering", IEEE Trans. on Automatic Control, 33(1), pp. 88-94, 1988.
14. Strobel, N., Spors, S. and Rabenstein, R., "Joint Audio-Video Object Localization and Tracking", IEE Signal Processin Magazine, pp.22-31, 2001.

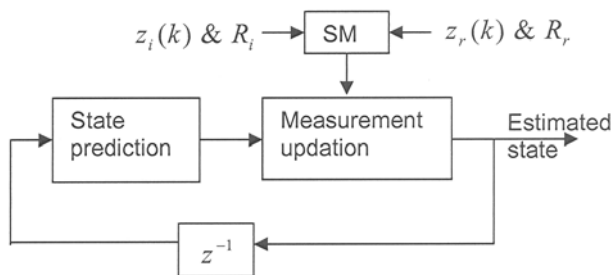


Fig.1 Information Flow Diagram of SM Algorithm

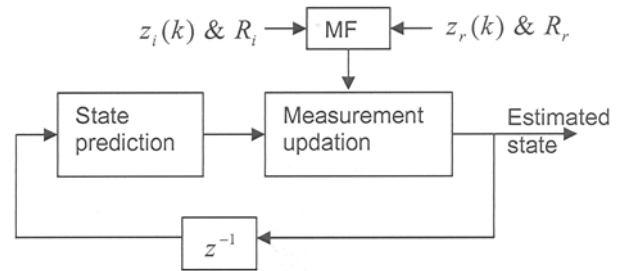


Fig.2 Information Flow Diagram of MF Algorithm

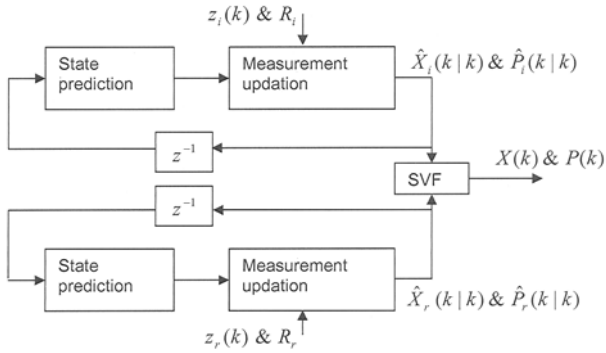


Fig.3 Information Flow Diagram of SVF Algorithm

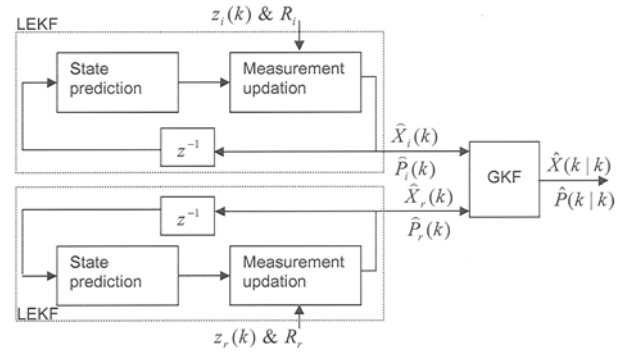


Fig.6 Information Flow Diagram of DKF Algorithm

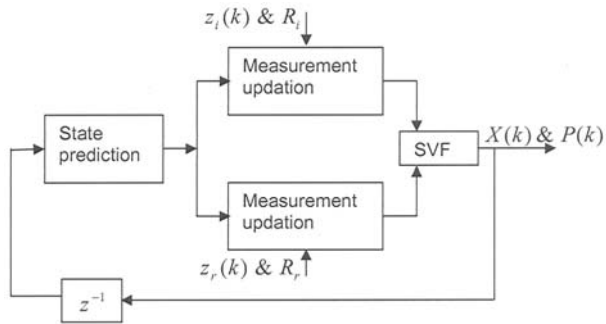


Fig.4 Information Flow Diagram of FSVF Algorithm

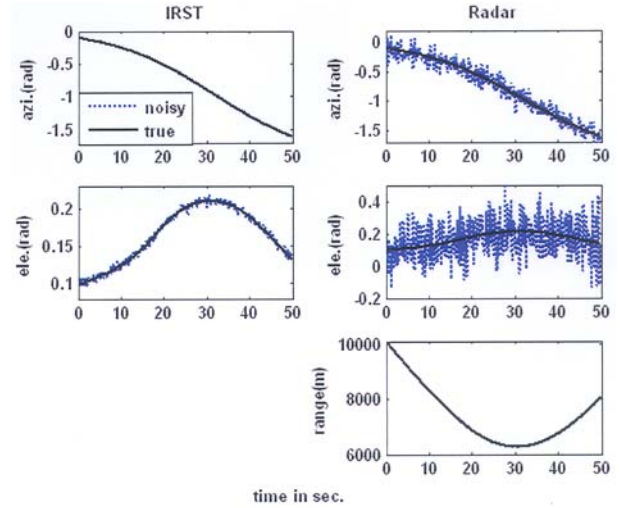


Fig.7 Noisy Measurements in Polar Coordinates

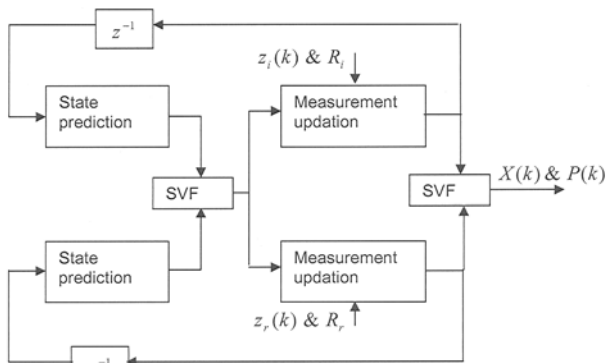


Fig.5 Information Flow Diagram of PSVF Algorithm

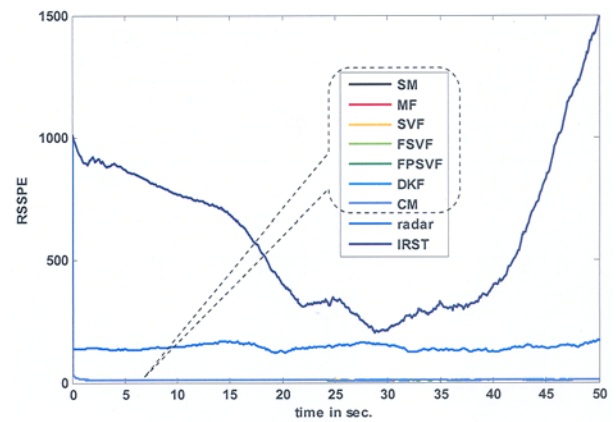


Fig.8a Root Sum Square Error in Position

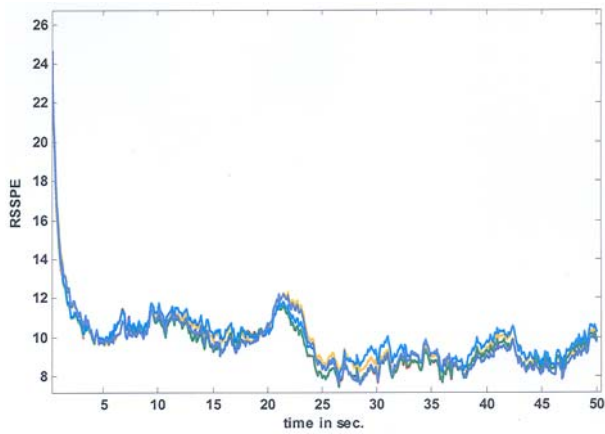


Fig.8b Zoomed View (y-axis) of Fig.8a

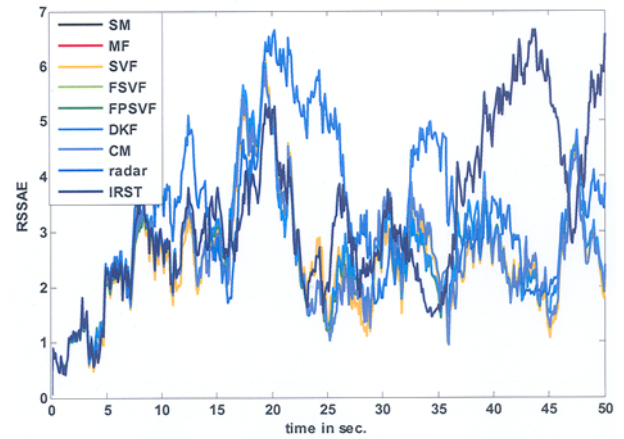


Fig.8e Root Sum Square Error in Acceleration

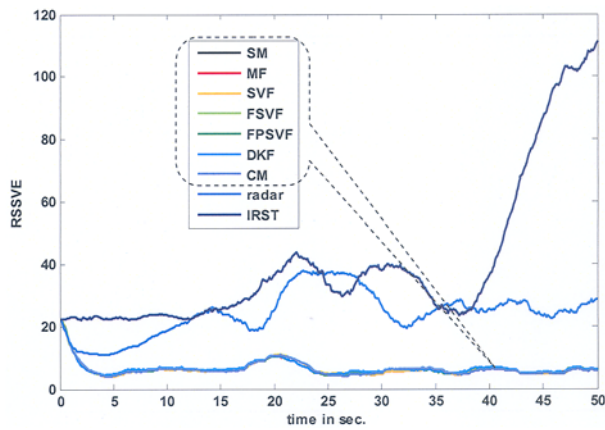


Fig.8c Root Sum Square Error in Velocity

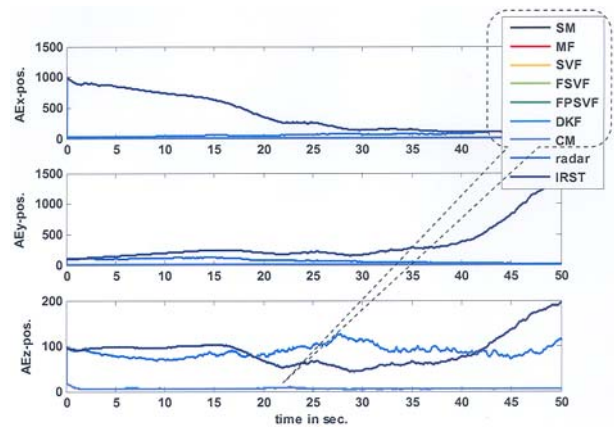


Fig.9a Absolute Error in Positions

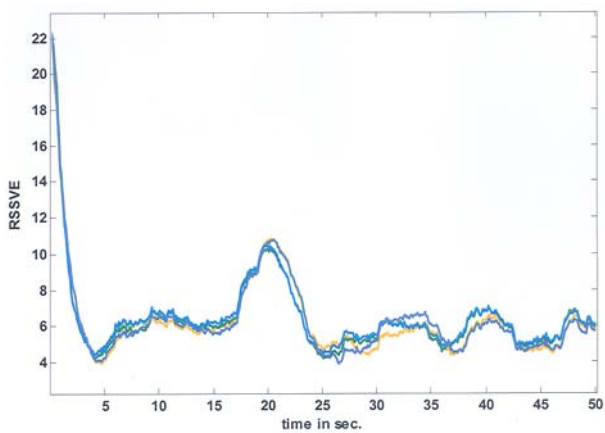


Fig.8d Zoomed View (y-axis) of Fig.8c

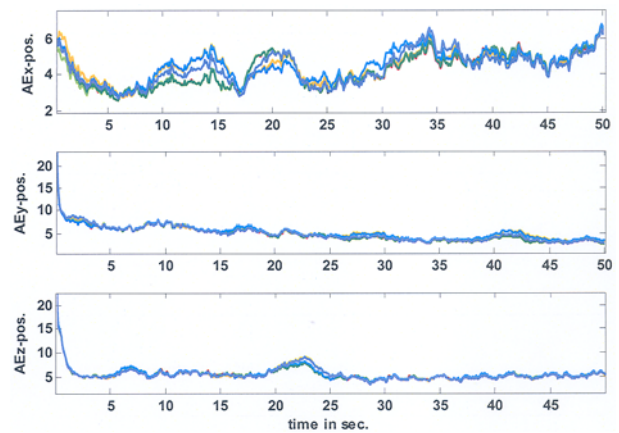


Fig.9b Zoomed View (y-axis) of Fig.9a

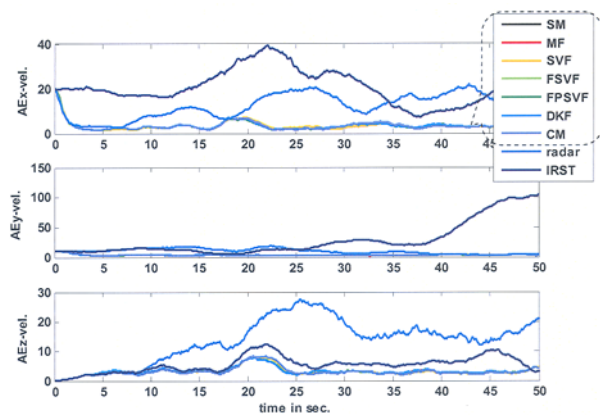


Fig.9c Absolute Error in Velocities

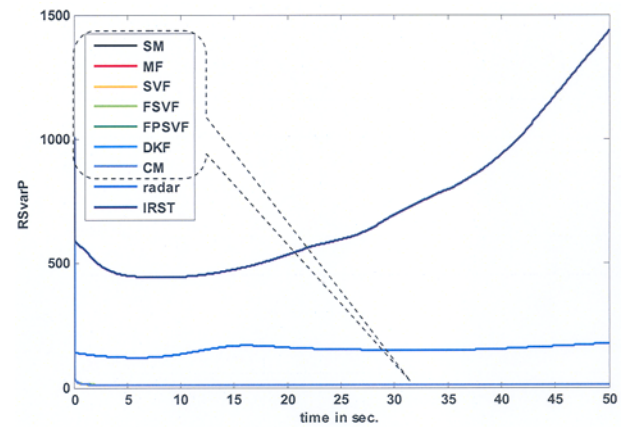


Fig.10a Root Sum Variance in Position

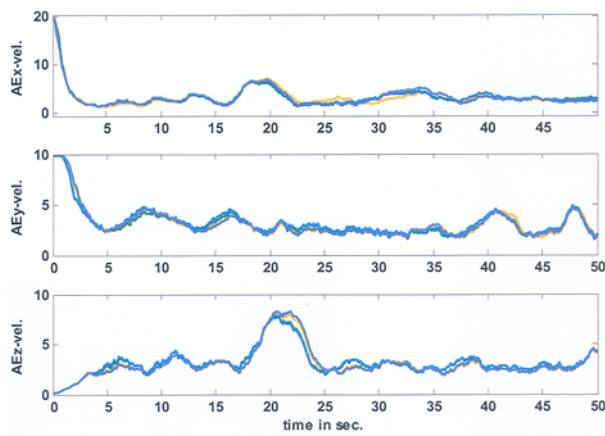


Fig.9d Zoomed View (y-axis) of Fig.9c

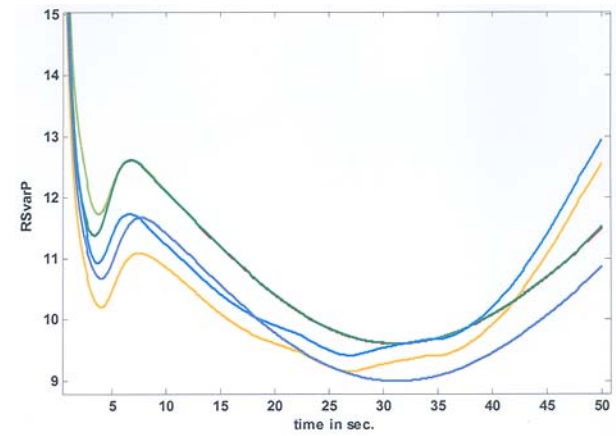


Fig.10b Zoomed View (y-axis) of Fig.10a

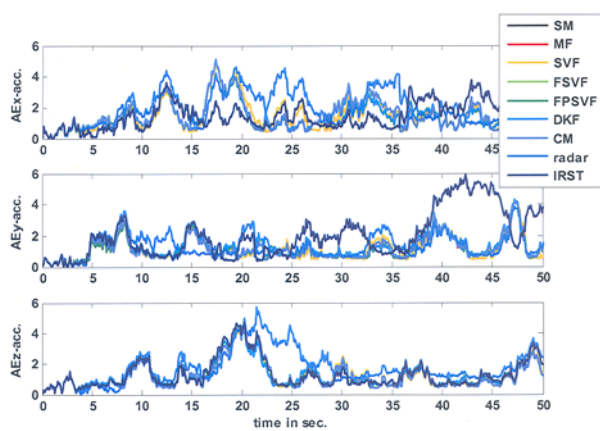


Fig.9e Absolute Error in Accelerations

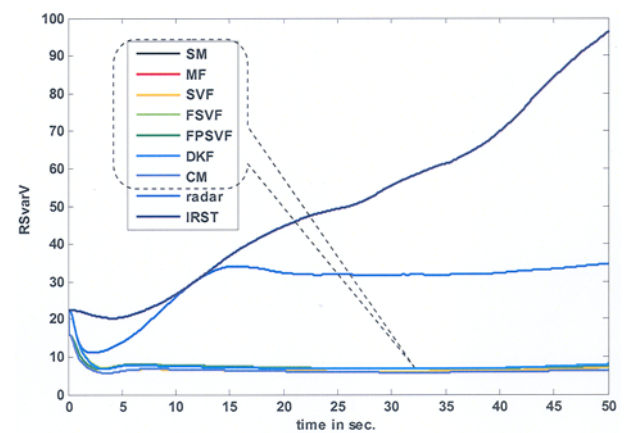


Fig.10c Root Sum Variance in Velocity

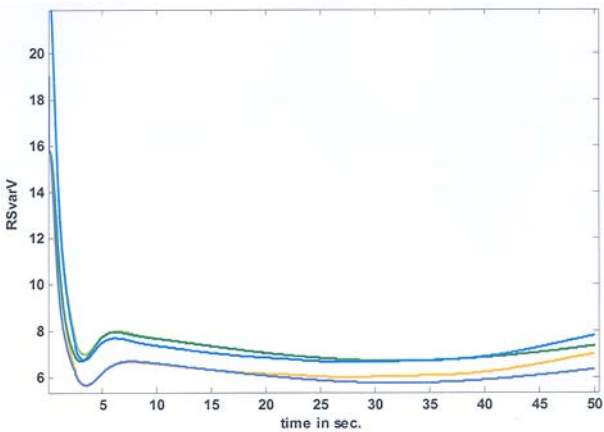


Fig.10d Zoomed View (y-axis) of Fig.10c

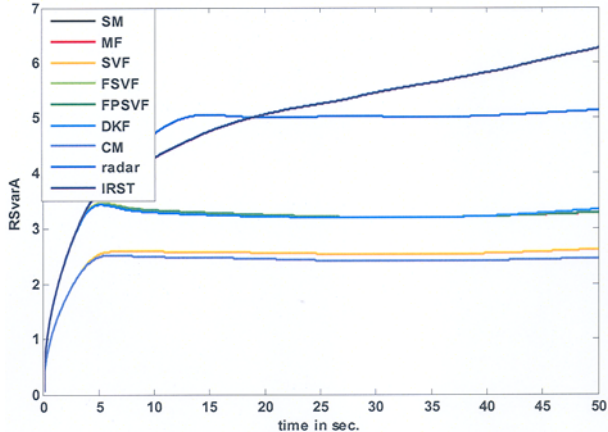


Fig.10e Root Sum Variance in Acceleration